



Published in final edited form as:

*J Med Chem.* 2013 February 28; 56(4): 1693–1703. doi:10.1021/jm301774u.

## Structural Modifications to Tetrahydropyridine-3-Carboxylate Esters en route to the Discovery of M<sub>5</sub>-Preferring Muscarinic Receptor Orthosteric Antagonists

Guangrong Zheng<sup>\*,†</sup>, Andrew M. Smith<sup>‡</sup>, Xiaoqin Huang<sup>‡</sup>, Karunai L. Subramanian<sup>‡</sup>, Kiran B. Siripurapu<sup>‡</sup>, Agripina Deaciuc<sup>‡</sup>, Chang-Guo Zhan<sup>‡</sup>, and Linda P. Dwoskin<sup>‡</sup>

<sup>†</sup>Department of Pharmaceutical Sciences, College of Pharmacy, University of Arkansas for Medical Sciences, Little Rock, Arkansas 72205

<sup>‡</sup>Department of Pharmaceutical Sciences, College of Pharmacy, University of Kentucky, Lexington, Kentucky 40536

### Abstract

The M<sub>5</sub> muscarinic acetylcholine receptor is suggested to be a potential pharmacotherapeutic target for the treatment of drug abuse. We describe herein the discovery of a series of M<sub>5</sub>-preferring orthosteric antagonists based on the scaffold of 1,2,5,6-tetrahydropyridine-3-carboxylic acid. Compound **56**, the most selective compound in this series, possesses an 11-fold selectivity for the M<sub>5</sub> over M<sub>1</sub> receptor, and shows little activity at M<sub>2</sub>–M<sub>4</sub>. This compound, although exhibiting modest affinity ( $K_i = 2.24 \mu\text{M}$ ) for the [<sup>3</sup>H]*N*-methylscopolamine binding site on the M<sub>5</sub> receptor, is potent (IC<sub>50</sub> = 0.45 nM) in inhibiting oxotremorine-evoked [<sup>3</sup>H]DA release from rat striatal slices. Further, a homology model of human M<sub>5</sub> receptor based on the crystal structure of the rat M<sub>3</sub> receptor was constructed, and docking studies of compounds **28** and **56** were performed in an attempt to understand the possible binding mode of these novel analogues to the receptor.

### INTRODUCTION

Muscarinic acetylcholine receptors (mAChRs<sup>a</sup>) are G-protein coupled receptors (GPCRs) activated by the endogenous neurotransmitter acetylcholine (ACh) and the natural alkaloid muscarine. Upon ACh activation, these receptors regulate a variety of central and peripheral physiological functions such as cognition, movement, sleep, cardiovascular function, smooth-muscle contractility, and glandular secretion.<sup>1–4</sup> Thus, mAChRs have emerged as important therapeutic targets for many diseases, such as Alzheimer's disease, Parkinson's disease, psychosis, pain, asthma, diabetes, and smooth-muscle disorders.<sup>3, 4</sup> Five mAChR subtypes (M<sub>1</sub>–M<sub>5</sub>) have been identified.<sup>2</sup> Each of the five mAChR subtypes has a defined distribution pattern within specific brain regions and peripheral tissues and mediates distinct physiological functions.<sup>1–4</sup> To avoid side effects, selectivity at specific mAChR subtypes is often a major focus of discovery of mAChR agonists and antagonists as therapeutic agents.

The M<sub>5</sub> mAChR was the last subtype to be cloned.<sup>2, 5</sup> A growing body of evidence suggests that this subtype is a potential target for the discovery of treatments for drug

\*Corresponding Author: Phone 501-526-6787; Fax 501-526-5945; gzheng@uams.edu.

The authors declare no conflict of financial interest.

Supporting Information

Synthetic procedures and analytical data of all compounds prepared. This material is available free of charge via the internet at <http://pubs.acs.org>.

abuse.<sup>6</sup> The rewarding effects of abused drugs are believed to be mediated by the mesolimbic dopamine (DA) pathway, which projects from the midbrain ventral tegmental area (VTA) to the nucleus accumbens.<sup>7–10</sup> M<sub>5</sub> mAChRs are the only muscarinic subtype localized to VTA and that modulate DA release from VTA DA neurons<sup>11–17</sup> Consistent with M<sub>5</sub> mAChR modulation of mesolimbic DA transmission, behavioral studies using M<sub>5</sub> knockout mice show a reduction in reward and withdrawal responses following repeated morphine or cocaine administration, as well as a reduction in the rate of cocaine self-administration.<sup>18–21</sup> Furthermore, microinfusion into VTA of an antisense oligonucleotide targeting M<sub>5</sub> receptor mRNA inhibits brain stimulation reward in rats<sup>15</sup> and microinfusion into the VTA of the nonselective mAChR antagonist, scopolamine (**1**, Figure 1), reduces cocaine-facilitated DA release in nucleus accumbens.<sup>17</sup> Microinfusion of the nonselective mAChR antagonist, atropine (**2**, Figure 1), into the VTA in rats dose-dependently inhibits morphine-induced conditioned place preference.<sup>22</sup> Taken together, these studies suggest that discovery of subtype-selective M<sub>5</sub> mAChR antagonists may provide novel treatments for drug abuse. Importantly, mice lacking M<sub>5</sub> receptors exhibit no difference from their wild-type littermates in various behavioral and pharmacologic tests,<sup>18,23</sup> suggesting that centrally-active M<sub>5</sub> receptor antagonists will be well tolerated.

Subtype-selective M<sub>5</sub> receptor antagonists also will be useful pharmacological tools in defining the physiological functions of this receptor. Currently, little information is available on the effects of selective activation or inhibition of M<sub>5</sub> receptors. Recent success in identifying M<sub>5</sub>-selective positive allosteric modulators may provide new information in this regard.<sup>24–26</sup> Nevertheless, no subtype-selective orthosteric M<sub>5</sub> antagonists are available to date. Unlike allosteric binding sites, which are usually more divergent across subtypes, orthosteric ACh binding sites across the five mAChR subtypes have been shown to be highly conserved at the amino acid sequence level (73–83% identity).<sup>5</sup> As such, selectivity among the mAChR subtypes is likely based on conformational dissimilarities, rather than upon single amino acid residues.<sup>27–29</sup> In fact, small molecule orthosteric antagonists with preference for an individual subtype have been reported for M<sub>1</sub>–M<sub>4</sub> but not M<sub>5</sub> (e.g., compound **3** for M<sub>1</sub>,<sup>30</sup> **5** for M<sub>2</sub>,<sup>31</sup> **6** for M<sub>3</sub>,<sup>32</sup> and **7** for M<sub>4</sub>,<sup>29</sup> Figure 1), indicating the existence of sufficient differences among the agonist recognition sites on the five mAChR subtypes allowing targeting of selective compounds to these sites.

Radioligand binding assays using membranes from recombinant cells expressing human mAChRs (hM<sub>1</sub>–hM<sub>5</sub>) show that compound **8** (1-ethyl-4-phenyl-1,2,5,6-tetrahydropyridine-3-carboxylic acid 4-methoxyphenethyl ester, Figure 1) preferentially binds to the M<sub>5</sub> receptor (subtype selectivity: M<sub>1</sub>/M<sub>5</sub> = 2.2-fold, M<sub>2</sub>/M<sub>5</sub> = 44-fold, M<sub>3</sub>/M<sub>5</sub> = 60-fold, M<sub>4</sub>/M<sub>5</sub> = 48-fold, Figure 1).<sup>33</sup> Thus, the current exploration of the structure activity relationship (SAR) regarding M<sub>5</sub> selective orthosteric ligands is based on compound **8**. To our best knowledge, compound **8** and its analogue **9** (Figure 1), are the only orthosteric small molecules reported to exhibit preference for M<sub>5</sub> receptors.<sup>33</sup>

The current structural modification strategy is provided in Figure 2. The 1,2,5,6-tetrahydropyridine-3-carboxylate core structure was retained, while modifying each part of the “appending” pharmacophores in a stepwise manner. These “appending” pharmacophores were to be rearranged around the core structure in compound **8** (Figure 2). Herein, we report the synthesis, pharmacological evaluation, and SAR analysis of this new series of mAChR antagonists. Additionally, a homology model of hM<sub>5</sub> mAChR was constructed based on the crystal structure of the rat M<sub>3</sub> mAChR. Preliminary docking experiments were performed using this model in an attempt to understand the structural basis of the interaction between these ligands and the receptor.

## RESULTS AND DISCUSSION

### Synthesis

The general synthetic methods for analogues **17–36** (Table 1) with modifications on the *p*-methoxyphenethyl moiety of compound **8** are depicted in Scheme 1. Transformation of commercially available ethyl 1-benzyl-4-oxo-3-piperidinecarboxylate (**11**) into compound **12** was achieved by initial conversion of **11** to *N*-BOC protected compound via a two-step process,<sup>34</sup> followed by triflation under diisopropylamine and trifluoromethanesulfonic anhydride.<sup>35</sup> Suzuki coupling of **12** with phenylboronic acid afforded compound **13**. Removal of BOC in **13** by TFA afforded compound **14**, which was then *N*-ethylated to form compound **15**. Compound **15** was subjected to ester hydrolysis under basic condition to afford carboxylic acid **16**. Treatment of **16** under a Steglich esterification condition with appropriate alcohols afforded **8** and its analogues **17–36**. The synthetic route for analogues with variations on the *N*-ethyl moiety of compound **8** was initially devised to introduce the *N*-substituent at the last step. Accordingly, compound **13** was converted to compound **38** in a sequence similar to that for compound **15** to **8** (Scheme 1). However, deprotection of **38** to form **39** using various de-BOC methods (TFA/CH<sub>2</sub>Cl<sub>2</sub>, HCl/EtOAc, AcCl/MeOH, or TsOH/CH<sub>2</sub>Cl<sub>2</sub>) resulted in complex mixtures. Attempts to purify compound **39** by silica gel column chromatography failed. Impure intermediate **39** (obtained from TFA treatment) was employed to provide *N*-Me, *N*-*n*-Pr, *N*-*n*-Bu, or *N*-*p*-methoxybenzyl analogues via reductive amination, but only *N*-*p*-methoxybenzyl analogue (compound **40**) was obtained in pure form after preparative TLC purification. Alternatively, a similar route to that for analogues **17–36** was applied to prepare analogues **42–59** from compound **14** (Scheme 1, Table 2).

Analogues **61–69** (Table 2) were synthesized in a similar manner to analogues **42–59** from triflate **12**. Phenyl ring substituted phenylboronic acids were used instead of phenylboronic acid as the Suzuki coupling partners (Scheme 2).

Analogues **70–73** were prepared by *N*-alkylation of compound **14** with appropriate alkyl halides (Scheme 3). Analogues **74–76** were prepared by reductive amination of compound **14** with an *N*-sulfonated or *N*-acylated 4-piperidinone using sodium triacetoxyborohydride (Scheme 3).

The synthesis of analogues **84** and **85** were initially attempted by applying a similar route to that used for the synthesis of their regioisomers in Scheme 1 (analogues **56** and **45**, respectively), starting from ethyl 1-benzyl-3-oxo-4-piperidinecarboxylate hydrochloride (**77**) (Scheme 4). However, de-BOC reaction of compound **78** failed to yield the desired intermediate **79**. As an alternative, analogues **84** and **85** were synthesized starting from 3-bromoisonicotinic acid (**80**). Ethyl esterification of **80** followed by Suzuki coupling with phenylboronic acid afforded compound **81**, which was treated with methyl iodide to yield the corresponding quaternary pyridinium salt **82**. Reduction of **82** with sodium borohydride gave 1,2,5,6-tetrahydropyridine derivative **83**, which underwent ester hydrolysis and subsequent esterification with appropriate alcohols to afford analogues **84** and **85**.

Synthesis of analogue **89** was achieved by initial Suzuki coupling of 4-bromopyridine with 2-(ethoxycarbonyl)phenylboronic acid, followed by a similar route to that for analogues **84** and **85** from compound **81** (Scheme 5).

### Radioligand Binding Assay

Receptor affinities were determined by measuring inhibition of the binding of [<sup>3</sup>H]*N*-methylscopolamine (NMS), an orthosteric antagonist probe, to membranes from Chinese hamster ovarian (CHO) cells individually expressing human hM<sub>1</sub>–hM<sub>5</sub> mAChR receptors.

Compound **1** (scopolamine) and compound **8** were used as reference compounds. Methods for these binding assays are described briefly in the Experimental Section. All synthesized analogues were evaluated first at hM<sub>1</sub> and hM<sub>5</sub> subtypes (Table 1 and 2, Scheme 3–5). Selectivity for M<sub>5</sub> over M<sub>1</sub> is important, because antagonism of CNS M<sub>1</sub> receptors has been suggested to result in cognitive deficits<sup>36</sup> and increase DA release in striatum.<sup>37</sup> Binding affinity for analogues which exhibited binding preference for M<sub>5</sub> over M<sub>1</sub> were determined at each of the five mAChR subtypes (Table 3).

Identification of compound **8** was the starting point. Compound **8** was an analogue of the 1-ethyl-4-phenyl-tetrahydropyridine-3-carboxylic acid scaffold aimed at identifying M<sub>1</sub> selective antagonists. Compound **8** was reported to have a 2.2-fold preference for M<sub>5</sub> over M<sub>1</sub>, and to be more than 40-fold selective for M<sub>5</sub> over M<sub>2</sub>–M<sub>4</sub> mAChR subtypes (Figure 1).<sup>33</sup> However, in the current study, compound **8** showed no selectivity for M<sub>5</sub> over M<sub>1</sub>–M<sub>4</sub> (Table 3). Preliminary SAR from the previous report<sup>33</sup> suggested that small changes on the *p*-methoxyphenyl ring of **8** afforded remarkably different binding affinity and selectivity profiles at mAChR subtypes. For example, when the methoxy group on the phenyl ring of **8** was replaced by a methyl group, the resulting analogue **10** bound preferentially to the M<sub>1</sub> receptor, while binding affinity at the M<sub>5</sub> receptor increased 35-fold, when compared to compound **8** (Figure 1).<sup>33</sup>

Results in Table 1 summarize the modifications to the *p*-methoxyphenethyl moiety of compound **8** evaluated in the current study and the influence of these modifications on binding affinity and selectivity for M<sub>1</sub> and M<sub>5</sub> receptors. Results from para-, meta-, and ortho-methoxy analogues, **8**, **17**, and **18**, respectively, indicate that the meta-substitution was favorable to M<sub>5</sub> selectivity. Compared to **8** ( $K_i = 420$  nM) and **17** ( $K_i = 1,250$  nM), meta-analogue (**18**,  $K_i = 150$  nM) exhibited a small 3- and 8-fold, respectively, increase in affinity at M<sub>5</sub> over M<sub>1</sub>. Replacement of the ethylene link in the *p*-methoxyphenethyl moiety by a methylene (compound **19**,  $K_i = 3,610$  nM) or a methyl ethylene link (compound **21**,  $K_i > 100$   $\mu$ M) significantly decreased binding potency at M<sub>5</sub> receptor, whereas replacement with a propylene link (compound **20**,  $K_i = 470$  nM) retained binding affinity at M<sub>5</sub> and markedly increased selectivity (7-fold) over M<sub>1</sub> receptors. Interestingly, there were no marked differences in M<sub>5</sub> affinities when the 4-methoxy was replaced with another para-substitution group, including halogens (compounds **23**–**25**) and nitro group (compound **26**), indicating modification at this position is somewhat tolerated. However, compound **27**, in which a 4-methylsulfonyl group was attached to the phenyl ring, exhibited little affinity for either M<sub>1</sub> or M<sub>5</sub> receptors. Compounds **28** and **31**, wherein both 3- and 4-positions of the phenyl ring were substituted, not only retained affinity at the M<sub>5</sub> receptor ( $K_i = 230$  and 2,460 nM, respectively), but also exhibited preference for this subtype (6.0- and 4.8-fold M<sub>5</sub>/M<sub>1</sub>, respectively). Tri-substitution of the phenyl ring in compounds **32** and **33** revealed that this modification was detrimental to binding. Finally, replacement of the 4-methoxyphenyl ring with a heterocyclic ring, including pyridyl (compounds **34** and **35**) and thiophenyl (compound **36**) rings, resulted in retention of binding affinity at both M<sub>1</sub> and M<sub>5</sub> receptors.

In parallel with the modification on the *p*-methoxyphenethyl group, the *N*-ethyl moiety of compound **8** (Table 2) also was altered. Replacement of the ethyl group by a methyl group (compound **42**) resulted in an 8-fold and 14-fold increase in binding affinity at M<sub>1</sub> and M<sub>5</sub> receptors, respectively. Increasing the size of the substituted group from ethyl to *n*-propyl (compound **43**), *n*-butyl (compound **44**), or 4-methoxybenzyl group (compound **40**) eliminated affinity for these two receptors. Similar results were observed for *N*-methyl, *N*-*n*-propyl, and *N*-*n*-butyl analogues (compounds **45**, **46**, and **47**, respectively) of compound **28**. Interestingly, the M<sub>1</sub>/M<sub>5</sub> selectivity of two *N*-methyl containing analogues, compound **42** (0.7-fold) or **45** (4.8-fold), were similar to their corresponding *N*-ethyl analogues, **8** (0.4-fold) and **28** (6.0-fold), respectively.

Based on the above SAR data, our focus changed to analogues bearing an *N*-methyl group in lieu of *N*-ethyl group, and the SAR was extended regarding the substitution group of the carboxylic ester moiety (Table 2). Replacement of the ethyl link in compound **45** by a methylene (compound **49**) or propylene (compound **50**) link resulted in a decrease in binding affinity at both M<sub>1</sub> and M<sub>5</sub> receptors, and also resulted in a decrease in selectivity for M<sub>5</sub> over M<sub>1</sub> receptors. SAR among compounds **45**, **49**, and **50** was inconsistent with previous SAR among compounds **8**, **19** and **20**, indicating an unpredictable nature of this component of the structure. On the other hand, analogues containing substituents at the meta-position or both the meta- and para-position of the ester phenyl ring (compounds **53–56**) consistently exhibited a binding preference at M<sub>5</sub> over M<sub>1</sub> receptor. Compound **56** was identified as the most selective (11-fold for M<sub>1</sub>/M<sub>5</sub>) M<sub>5</sub> compound.

Based on compounds **45** and **56**, SAR was further extended by introduction of an electron-withdrawing (fluoro) or electron-donating (methoxy) group onto the phenyl ring on the C4 of the tetrahydropyridine core (compounds **61–69**, Table 2). In general, these analogues exhibited decreased or completely abolished activity at either M<sub>1</sub> or M<sub>5</sub> receptor when compared to compound **45** and **56**, suggesting that this component of the molecule is less tolerant to structural modification.

Further SAR exploration was focused on previous hypotheses that spatial rearrangement or reorientation of the pharmacophore elements in mAChR ligands would alter affinity and selectivity profiles.<sup>38</sup> For example, rearrangement of the amino group in M<sub>1</sub> preferring antagonist **3** (pirenzepine) afforded M<sub>2</sub> preferring antagonist **4** (Figure 1).<sup>39</sup> To test this hypothesis with respect to the current analogues, we conducted three types of pharmacophoric “rearrangements”. First, transposition of the substituted group on the ester functionality and the ethyl group on the *N* atom in compound **8** and analogues afforded compounds **70–73** (Scheme 3). An *N*-acylated or *N*-sulfonated piperidine-4-yl group also was introduced to the *N* atom of the tetrahydropyridine ring (compounds **74–76**, Scheme 3). The *N*-substituents were selected because they are present in potent mAChR orthosteric antagonists, such as darifenacin (**90**), zamifenacin (**91**), and compounds **92** and **93**<sup>40</sup> (Figure 3). Surprisingly, none of these new analogues displayed any activity at either M<sub>1</sub> or M<sub>5</sub> receptors, indicating a different receptor binding mode for the basic *N* atom in compound **8** and its analogues compared with compounds **90–93**.

Second, the ester group on C3 and the phenyl group on C4 of the 1,2,5,6-tetrahydropyridine ring in compounds **56** and **45** were transposed to produce compounds **84** and **85** (Scheme 4), respectively. Both compounds **84** (M<sub>1</sub>/M<sub>5</sub> = 2.4) and **85** (M<sub>1</sub>/M<sub>5</sub> = 2.1) displayed reduced selectivity for M<sub>5</sub> over M<sub>1</sub> receptors, when compared to their corresponding position isomers, **56** and **45**, respectively. Last, the ester functionality in compound **45** was moved from C3 of the tetrahydropyridine ring to the phenyl ring on C4 (compound **89**, Scheme 5). This “parallel” shift resulted in a complete loss of binding affinity at both M<sub>1</sub> and M<sub>5</sub> receptors.

At saturation concentrations, all analogues, except for those with  $K_i > 100,000$  nM, exhibited complete inhibition (maximal inhibition,  $I_{\max} = 100\%$ , data not show) of the binding of the orthosteric antagonist [<sup>3</sup>H]NMS at mAChRs, which is consistent with an orthosteric mechanism of action. Selected compounds, including **20**, **28**, **45**, **56**, **57**, **63**, and **66**, which exhibited binding preference for hM<sub>5</sub> over hM<sub>1</sub> mAChRs, also were evaluated for affinity at M<sub>2</sub>, M<sub>3</sub>, and M<sub>4</sub> mAChR subtypes (Table 3). Results showed that 5 of these 7 compounds exhibited good selectivity for M<sub>5</sub> over M<sub>2</sub>, M<sub>3</sub>, and M<sub>4</sub> receptors. The most selective compound, **56** (11-fold for M<sub>5</sub> over M<sub>1</sub> receptor), had no affinity ( $K_i > 100$  μM) at the M<sub>2</sub>, M<sub>3</sub>, and M<sub>4</sub> mAChR subtypes. Compound **28** exhibited 6-fold, >435-fold, 135-fold, and 46-fold for M<sub>5</sub> over M<sub>1</sub>, M<sub>2</sub>, M<sub>3</sub>, and M<sub>4</sub>, respectively. Although slightly less

selective for the M<sub>5</sub> over the M<sub>1</sub> receptor, it exhibited higher affinity at M<sub>5</sub> when compared to compound **56**.

### Inhibition of Oxotremorine-Evoked Striatal [<sup>3</sup>H]DA Release

*In vitro* functional assays for mAChR antagonists measure the ability of molecules to block mAChR agonist-induced receptor activation at recombinant mAChR subtypes expressed in cells.<sup>41</sup> Pharmacological studies of M<sub>5</sub> receptors using mouse basilar artery also have been reported.<sup>42</sup> However, these recombinant and native M<sub>5</sub> receptors functional assays are far removed from a potential role for M<sub>5</sub> receptors in cocaine and opiate addiction. Studies have shown that oxotremorine, a non-selective mAChR agonist, concentration dependently increases [<sup>3</sup>H]DA release from striatal slices prepared from wild-type mice and that oxotremorine-evoked striatal [<sup>3</sup>H]DA release was reduced significantly in M<sub>5</sub> receptor knockout mice.<sup>18, 43</sup> We hypothesized that an M<sub>5</sub> receptor selective antagonist would also reduce oxotremorine-mediated rat striatal [<sup>3</sup>H]DA release. Current results show that oxotremorine evokes [<sup>3</sup>H]DA release from rat striatal slices and that scopolamine inhibits this effect in a concentration-dependent manner (Figure 4). These results support the contention that this functional assay probes native M<sub>5</sub> receptors. Furthermore, this functional assay is highly relevant to the underlying dopaminergic mechanisms involved in drug reward and abuse.

Results revealed that compound **56** inhibited (IC<sub>50</sub> = 0.45 nM) oxotremorine (100 μM) evoked [<sup>3</sup>H]DA release from rat striatal slices (Figure 5). Unlike scopolamine (1 μM), which completely inhibits oxotremorine-mediated [<sup>3</sup>H]DA release from rat striatal slices (Figure 4), compound **56** produced maximal inhibition (I<sub>max</sub>) of only 48% of the oxotremorine-evoked [<sup>3</sup>H]DA release (Figure 5). These current results are consistent with previous reports that ~50% of oxotremorine-evoked [<sup>3</sup>H]DA release from striatal slices was eliminated in M<sub>5</sub> knock-out mice compared to wild-type mice,<sup>18</sup> indicating that other mAChR subtype(s) also mediate oxotremorine-evoked striatal DA release. In agreement with this hypothesis, studies using mAChR knock-out mice suggested that M<sub>3</sub> and M<sub>4</sub> receptors also were involved in mediating striatal DA release.<sup>43</sup> The observations that both compound **56** and the deletion of the M<sub>5</sub> receptor resulted in similar effects on oxotremorine-evoked striatal [<sup>3</sup>H]DA release, together with the selective binding of **56** to M<sub>5</sub> over M<sub>3</sub> and M<sub>4</sub> receptors, strongly suggest that **56** interacts with M<sub>5</sub> receptors to inhibit muscarinic agonist-induced striatal DA release.

It is noteworthy that compound **56** (IC<sub>50</sub> = 0.45 nM) appears more potent than scopolamine in inhibiting oxotremorine-evoked [<sup>3</sup>H]DA release from rat striatal slices although its [<sup>3</sup>H]NMS binding affinity on the M<sub>5</sub> receptor is 127-fold less than scopolamine. One explanation on the lack of correlation between binding and function is that the [<sup>3</sup>H]NMS binding assay was performed on a single receptor in a recombinant system but the [<sup>3</sup>H]DA release assay was on heterogeneous brain slices. Compound **56** may potentially act at other sites that also inhibit [<sup>3</sup>H]DA release. Alternatively, recent studies on the crystal structure of the rat M<sub>3</sub> receptor with antagonist tiotropium bound to the orthosteric binding site suggested that tiotropium binds transiently to an allosteric site en route to the orthosteric binding pocket.<sup>44</sup> Compound **56** could have a similar allosteric interaction with the receptor, causing the inhibition of oxotremorine-evoked striatal [<sup>3</sup>H]DA release. However, further pharmacological studies are needed to elucidate the mechanism.

### Binding Mode for M<sub>5</sub> mAChRs for Lead Compounds **28** and **56**

To study the interaction of our compounds with M<sub>5</sub> mAChR in atomic detail, homology modeling and molecular docking operations were performed. Compounds **28** and **56** were selected for these studies, since both analogues preferentially bind to M<sub>5</sub> mAChR, and

thus, can be considered current lead compounds. Importantly, compounds **28** and **56** have an order of magnitude difference in binding affinities at M<sub>5</sub> receptor ( $K_i = 230$  nM vs 2240 nM, respectively). This moderate difference in affinity between **28** and **56** is ideal for testing the reliability of our homology models. The structural model of the human M<sub>5</sub> mAChR was constructed based on the newly available X-ray crystal structure of the rat M<sub>3</sub> mAChR with antagonist tiotropium bound to the orthosteric binding site.<sup>44</sup> Compounds **28** and **56** were docked into possible binding sites among the transmembrane (TM) helices of the M<sub>5</sub> mAChR. Binding structures were selected from the docking results and subjected to energy minimization. In accordance with the minimized binding structures, the binding site for compounds **28** and **56** at the M<sub>5</sub> mAChR is the orthosteric site located near the extracellular end of TM3, TM5, TM6, and TM7. As shown in Figure 6, TM2 and TM4 are also partially involved in the formation of the antagonist-binding site. In addition, the antagonist binding site is partially covered by extracellular loop 2 (EL-2). As depicted in Figure 6A, compound **28** is orientated horizontally inside the binding pocket. The cationic head of compound **28** is anchored around the negatively charged side chain of residue D110 of TM3, interacting through electrostatic attraction and strong hydrogen bonding. Meanwhile, residue D110 is also hydrogen-bonded with the side chain of S83 from TM2, and the side chains of Y481 and Y485 from TM7. The cationic head of compound **28** is in close contact with residues W106 and L107 from TM3. The phenyl group on C4 of tetrahydropyridine ring is closely packed with Y87, Y90 and I91 from TM2, W106 from TM3, F187 from EL-2, and H478 from TM7. The ethyl group at the cationic head of compound **28** contacts with the aromatic side chain of residue F82 from TM2. The carbonyl oxygen of compound **28** is weakly hydrogen-bonded with the hydroxyl group at the side chain of Y458 from TM6. The tail group (2,3-dihydrobenzofuran-5-ethyl) of compound **28** is packed in parallel with the underneath Y111 from TM3, and packed perpendicularly with the side chain of W162 from TM4. The tail group of compound **28** is also surrounded by T197 from TM5 and V462 from TM6.

As depicted in Figure 6B, the binding mode of the M<sub>5</sub> mAChR with compound **56** is essentially the same as that with compound **28**. One difference between the binding of **56** and **28** to the M<sub>5</sub> mAChR is that residues I193 and T194 from TM5 are both within 5 Å of compound **56** (Figure 6B), while these two residues have no contacts with compound **28** (Figure 6A). Another difference is the distance of hydrogen bonding formed by the side chain of residue D110 with the cationic head group of the antagonist. As shown in Figure 6, the distance between the hydrogen bonding between residue D110 and the cationic head of compound **28** is shorter than that of the hydrogen bonding between residue D110 and the cationic head of compound **56** (1.93 Å vs 1.99 Å, respectively), indicating a stronger bond with **28** than with **56** to the protein. These structural differences, especially the difference in hydrogen bonding distance, may contribute to the difference in binding affinity as represented by the experimentally measured values of  $K_i$  (230 nM for **28** vs. 2240 nM for **56**) for these two lead compounds (Table 3). The modeled binding structures helped to qualitatively understand the observed SAR and provided clues to design a valuable virtual library of new analogues for computational screening.

## SUMMARY

Starting from compound **8** as a lead structure, we have identified the first M<sub>5</sub>-preferring antagonists through a systematic structural modification strategy. The greatest mAChR selectivity and potency shifts came from the modification of the substituents on the ester group. Replacing the *N*-Et group on the tetrahydropyridine ring with an *N*-Me group generally resulted in a significant increase in mAChR binding affinity, while maintaining mAChR subtype-selectivity profile. This preliminary SAR study provides a basis for further discovery of potent and selective M<sub>5</sub> ligands. In addition, we have successfully

established a functional assay for M<sub>5</sub> receptors using oxotremorine-evoked DA release from superfused rat striatal slices. One of our lead compound, **56**, demonstrated inhibition of oxotremorine-mediated striatal [<sup>3</sup>H]DA release, with a maximal inhibition of ~50%. This result is similar to the effects of M<sub>5</sub> knock-out on striatal [<sup>3</sup>H]DA release, providing validation for the current assay. Further, we have constructed a homology model of human M<sub>5</sub> based on the newly available crystal structure of the rat M<sub>3</sub> receptor. Docking studies performed on compounds **28** and **56** revealed that both possibly interact with the orthosteric binding site on the M<sub>5</sub> receptor, which is consistent with the current results from the [<sup>3</sup>H]NMS binding assay, indicating an orthosteric mechanism of action for these new analogues. We are building and validating homology models for the other four mAChR subtypes, and these will be used for virtual library screening. The predictability of these models regarding mAChR subtype selectivity remains to be tested.

## EXPERIMENTAL SECTION

### Chemistry

All purchased reagents and solvents were used without further purification unless otherwise noted. All reaction sensitive to air and/or moisture were carried out under argon atmosphere in oven-dried glassware. Flash column chromatography was carried out using 32–63 μm, 60 Å (230–400 mesh) silica gel. Analytical thin layer chromatography was carried out on glass plates precoated with 250 μm silica gel 60 F<sub>254</sub>. NMR spectra were recorded in CDCl<sub>3</sub> on a Varian 300 MHz or 500 MHz spectrometer and chemical shifts are reported in ppm relative to tetramethylsilane as the internal standard. Coupling constants are reported in Hertz (Hz). Mass spectra were recorded on a JEOL JMS-700T MStation. GC-Mass spectra were recorded on an Agilent 6890 GC incorporating an Agilent 7683 autosampler and an Agilent 5973 MSD. Elemental analyses were carried out on a COSTECH elemental combustion system and are within ± 0.4% of theory. All final compounds for biological testing were prepared as salts in 95% purity, in accord with results from combustion analysis. A detailed description of synthetic methodologies as well as analytical and spectroscopic data for all described compounds is included in the Supporting Information.

### Binding Assay

Analogue binding affinities for the five mAChR subtypes were determined in assays evaluating inhibition of [<sup>3</sup>H]NMS binding to membranes from CHO-K1 cells expressing one of the recombinant hM<sub>1</sub>–hM<sub>5</sub> mAChRs. The CHO-K1 cell lines expressing the five subtypes of muscarinic receptors were obtained as a gift from Dr. Tom Bonner of National Institute of Mental Health (NIMH). Cells were grown at 37 °C with 5% CO<sub>2</sub> in Dulbecco's modified Eagle's medium (DMEM) supplemented with 10% fetal bovine serum, 4 mM glutamine, 50 ng/mL geneticin G418 and 1% Pen-Strep. Cells were harvested at 70–90% confluency. To obtain cell membranes, cells were scraped into ice cold 50 mM Tris-HCl (pH 7.4), sonicated for 30 s and centrifuged (48,000 g for 30 min). Pellets were re-suspended in 1.5 ml ice-cold 50 mM Tris-HCl buffer, sonicated for 30 s and stored at –80 °C until assay. Assays were performed using 96-well plates. Membrane aliquots (100 μL) containing 10–40 μg protein were added to wells containing 1 nM to 100 μM of test compound (25 μL), 0.3 nM [<sup>3</sup>H]NMS (25 μL; scopolamine methyl chloride [N-methyl-3H]; specific activity 82 Ci/mmol; Perkin Elmer/NEN, Boston, MA) and buffer (50 mM Tris-HCl, pH 7.4; 125 μL) for a total volume of 250 μL. Atropine (1 mM) was used to determine nonspecific binding. Samples were incubated for 120 min at 25 °C with constant agitation. Reactions were terminated by rapid filtration onto GF/B filters using a Filtermate Harvester (Perkin Elmer Life and Analytical Sciences, Boston, MA). Samples were washed three times with 350 μL of ice-cold 50 mM Tris-HCl buffer, and dried for 60 min at 50 °C. Subsequently, 40 μL MicroScint 20 (PerkinElmer Life and Analytical Sciences, Waltham,



MA) was added to each well and radioactivity bound determined using liquid scintillation spectrometry. IC<sub>50</sub> values were obtained and K<sub>i</sub> values calculated using the equation of Cheng and Prusoff.<sup>45</sup>

### Inhibition of Oxotremorine-Evoked [<sup>3</sup>H]DA Release Assay

Assays were performed according to previously published methods,<sup>47</sup> with minor modifications. Striata were dissected, and coronal slices (500 μm, 4–6 mg) obtained with a McIlwain chopper. Slices were incubated for 30 min in Krebs' buffer (in mM: 108 NaCl, 4.7 KCl, 1.2 MgCl<sub>2</sub>, 1 NaH<sub>2</sub>PO<sub>4</sub>, 1.3 CaCl<sub>2</sub>, 11.1 glucose, 25 NaHCO<sub>3</sub>, 0.11 L-ascorbic acid and 0.004 disodium EDTA, pH 7.4, saturated with 95% O<sub>2</sub>/5% CO<sub>2</sub>) in a metabolic shaker at 34°C. Slices were incubated with 0.1 μM [<sup>3</sup>H]DA during the latter 30 min of a 60-min incubation period. Each slice was transferred to a superfusion chamber and superfused (0.6 mL/min at 34 °C) for 60 min with Krebs' buffer containing nomifensine (10 μM) and pargyline (10 μM) to inhibit reuptake and prevent metabolism, respectively, ensuring that [<sup>3</sup>H]overflow primarily represents [<sup>3</sup>H]DA, rather than [<sup>3</sup>H]metabolites.<sup>47</sup> Sample collection began after 60 min of superfusion, when the rate of release was stable. Consecutive 4-min (2.4 mL) samples were collected to determine basal [<sup>3</sup>H]outflow. Superfusion continued in the absence or presence of a range of analogue concentrations (0.1 nM – 1 mM) for 40 min, followed by 40 min with oxotremorine (100 μM) added to the superfusion buffer. Radioactivity in slices and superfusate samples were determined via liquid scintillation spectroscopy. Data were analyzed by weighted, least squares regression analysis of the sigmoidal concentration-effect curves to obtain IC<sub>50</sub> values.

### Homology Modeling and Molecular Docking

The homology model of human M<sub>5</sub> mAChR was built based on the X-ray crystal structure of rat M<sub>3</sub> mAChR (PDB entry of 4DAJ at 3.4 Å resolution, A chain)<sup>44</sup> by using the Protein Modeling module of Discovery Studio (version 2.5.5, Accelrys, Inc. San Diego, CA). The model of human M<sub>5</sub> mAChR structure was constructed and refined in a very similar manner as in our previous study,<sup>48</sup> i.e. the best sequence alignment was selected based on both the alignment score and the reciprocal positions of the conserved residues among all mAChR subtypes. The coordinates of the conserved regions were directly transformed from the template structure, while the non-conserved residues were mutated from the template to the corresponding ones in M<sub>5</sub> mAChR. Structural optimization and energy minimization for the M<sub>5</sub> mAChR structure were performed using the Amber 11 program suite. The convergence criterion for the energy minimization was set to 0.001 kcal mol<sup>-1</sup> Å<sup>-1</sup>. Based on the optimized M<sub>5</sub> mAChR structure, the binding mode of the receptor with two lead compounds **28** and **56** was explored through molecular docking using AutoDock 3.0.5 program.<sup>48</sup> This molecular docking approach was similar to that described in our previous study.<sup>49</sup> A reasonable binding structure of M<sub>5</sub> mAChR in complex with either compound **28** or **56** was obtained after energy minimization on each complex structure.

### Supplementary Material

Refer to Web version on PubMed Central for supplementary material.

### Acknowledgments

This work was supported financially by a Pilot Project Grant from Center for Drug Abuse Research Translation at the University of Kentucky (DA05312) and grants from National Institute of Drug Abuse, National Institute of Health (DA025948, DA030667 and TR000117).

## ABBREVIATIONS

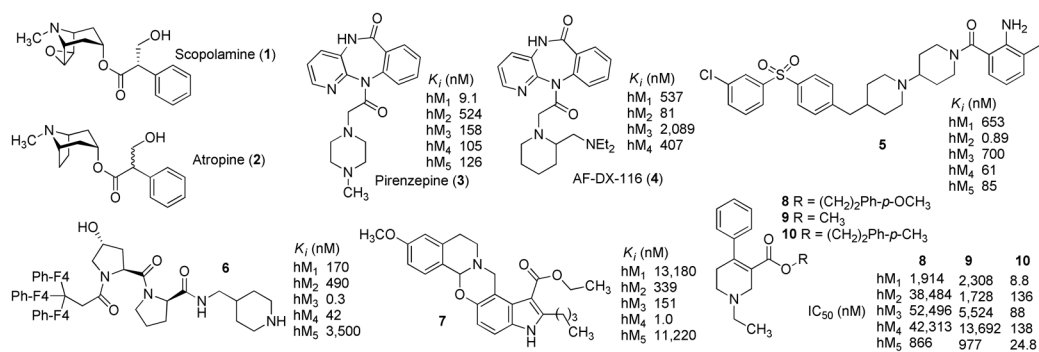
<b>VTA</b>	ventral tegmental area
<b>NMS</b>	<i>N</i> -methylscopolamine
<b>CHO</b>	Chinese hamster ovarian
<b>TM</b>	transmembrane
<b>EL</b>	extracellular loop

## References

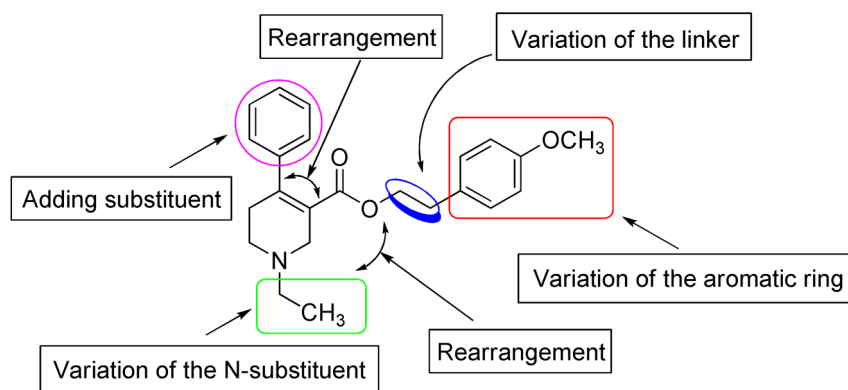
1. Caulfield MP. Muscarinic receptors - characterization, coupling and function. *Pharmacol Therapeut.* 1993; 58:319–379.
2. Caulfield MP, Birdsall NJ. International Union of Pharmacology. XVII. Classification of muscarinic acetylcholine receptors. *Pharmacol Rev.* 1998; 50:279–290. [PubMed: 9647869]
3. Wess J. Muscarinic acetylcholine receptor knockout mice: novel phenotypes and clinical implications. *Annu Rev Pharmacol Toxicol.* 2004; 44:423–450. [PubMed: 14744253]
4. Wess J, Eglén RM, Gautam D. Muscarinic acetylcholine receptors: mutant mice provide new insights for drug development. *Nat Rev Drug Discov.* 2007; 6:721–733. [PubMed: 17762886]
5. Bonner TI, Young AC, Brann MR, Buckley NJ. Cloning and expression of the human and rat M<sub>5</sub> muscarinic acetylcholine-receptor genes. *Neuron.* 1988; 1:403–410. [PubMed: 3272174]
6. Raffa RB. The M<sub>5</sub> muscarinic receptor as possible target for treatment of drug abuse. *J Clin Pharm Ther.* 2009; 34:623–629. [PubMed: 20175795]
7. Di Chiara G, Imperato A. Drugs abused by humans preferentially increase synaptic dopamine concentrations in the mesolimbic system of freely moving rats. *Proc Natl Acad Sci U S A.* 1988; 85:5274–5278. [PubMed: 2899326]
8. Koob GF, Swerdlow NR. The functional output of the mesolimbic dopamine system. *Ann N Y Acad Sci.* 1988; 537:216–227. [PubMed: 3059925]
9. Koob GF, Nestler EJ. The neurobiology of drug addiction. *J Neuropsychiatry Clin Neurosci.* 1997; 9:482–497. [PubMed: 9276849]
10. Cami J, Farre M. Drug addiction. *N Engl J Med.* 2003; 349:975–986. [PubMed: 12954747]
11. Vilaro MT, Palacios JM, Mengod G. Localization of M<sub>5</sub> muscarinic receptor messenger-RNA in rat-brain examined by in situ hybridization histochemistry. *Neurosci Lett.* 1990; 114:154–159. [PubMed: 2395528]
12. Yasuda RP, Ciesla W, Flores LR, Wall SJ, Li M, Satkus SA, Weisstein JS, Spagnola BV, Wolfe BB. Development of antisera selective for M<sub>4</sub> and M<sub>5</sub> muscarinic cholinergic receptors-distribution of M<sub>4</sub> and M<sub>5</sub> receptors in rat-brain. *Mol Pharmacol.* 1993; 43:149–157. [PubMed: 8429821]
13. Weiner DM, Brann MR. Distribution of M<sub>1</sub>-M<sub>5</sub> muscarinic receptor messenger-RNAs in rat-brain. *Trends Pharmacol Sci.* 1989:115–115.
14. Reever CM, FerrariDiLeo G, Flynn DD. The M<sub>5</sub> (m5) receptor subtype: fact or fiction? *Life Sci.* 1997; 60:1105–1112. [PubMed: 9121354]
15. Yeomans JS, Takeuchi J, Baptista M, Flynn DD, Lepik K, Nobrega J, Fulton J, Ralph MR. Brain-stimulation reward thresholds raised by an antisense oligonucleotide for the M<sub>5</sub> muscarinic receptor infused near dopamine cells. *J Neurosci.* 2000; 20:8861–8867. [PubMed: 11102495]
16. Miller AD, Blaha CD. Midbrain muscarinic receptor mechanisms underlying regulation of mesoaccumbens and nigrostriatal dopaminergic transmission in the rat. *Eur J Neurosci.* 2005; 21:1837–1846. [PubMed: 15869479]
17. Lester DB, Miller AD, Blaha CD. Muscarinic receptor blockade in the ventral tegmental area attenuates cocaine enhancement of laterodorsal tegmentum stimulation-evoked accumbens dopamine efflux in the mouse. *Synapse.* 2010; 64:216–223. [PubMed: 19862686]

18. Yamada M, Lamping KG, Duttaroy A, Zhang WL, Cui YH, Bymaster FP, McKinzie DL, Felder CC, Deng CX, Faraci FM, Wess J. Cholinergic dilation of cerebral blood vessels is abolished in M<sub>5</sub> muscarinic acetylcholine receptor knockout mice. *Proc Natl Acad Sci U S A*. 2001; 98:14096–14101. [PubMed: 11707605]
19. Basile AS, Fedorova I, Zapata A, Liu X, Shippenberg T, Duttaroy A, Yamada M, Wess J. Deletion of the M<sub>5</sub> muscarinic acetylcholine receptor attenuates morphine reinforcement and withdrawal but not morphine analgesia. *Proc Natl Acad Sci U S A*. 2002; 99:11452–11457. [PubMed: 12154229]
20. Fink-Jensen A, Sorensen L, Bay-Richter C, Frikke-Schmidt H, Wess J, Woldbye DP, Wortwein G. Involvement of the M<sub>5</sub> muscarinic receptor in cocaine and amphetamine induced behaviour: Studies in M<sub>5</sub> knockout mice backcrossed to the C57BL/6NTac strain. *Schizophrenia Research*. 2006; 81:301–302. [PubMed: 16256309]
21. Thomsen M, Woldbye DPD, Wortwein G, Fink-Jensen A, Wess J, Caine SB. Reduced cocaine self-administration in muscarinic M-5 acetylcholine receptor-deficient mice. *J Neurosci*. 2005; 25:8141–8149. [PubMed: 16148222]
22. Rezayof A, Nazari-Serenjeh F, Zarrindast MR, Sepehri H, Delphi L. Morphine-induced place preference: involvement of cholinergic receptors of the ventral tegmental area. *Eur J Pharmacol*. 2007; 562:92–102. [PubMed: 17336285]
23. Yamada M, Basile AS, Fedorova I, Zhang WL, Duttaroy A, Cui YH, Lamping KG, Faraci FM, Deng CX, Wess J. Novel insights into M-5 muscarinic acetylcholine receptor function by the use of gene targeting technology. *Life Sci*. 2003; 74:345–353. [PubMed: 14607263]
24. Bridges TM, Marlo JE, Niswender CM, Jones CK, Jadhav SB, Gentry PR, Plumley HC, Weaver CD, Conn PJ, Lindsley CW. Discovery of the First Highly M<sub>5</sub>-Preferring Muscarinic Acetylcholine Receptor Ligand, an M<sub>5</sub> Positive Allosteric Modulator Derived from a Series of 5-Trifluoromethoxy N-Benzyl Isatins. *J Med Chem*. 2009; 52:3445–3448. [PubMed: 19438238]
25. Bridges TM, Kennedy JP, Cho HP, Breining ML, Gentry PR, Hopkins CR, Conn PJ, Lindsley CW. Chemical lead optimization of a pan G(q) mAChR M-1, M-3, M-5 positive allosteric modulator (PAM) lead. Part I: Development of the first highly selective M-5 PAM. *Bioorg Med Chem Lett*. 2010; 20:558–562. [PubMed: 20004578]
26. Bridges TM, Kennedy JP, Hopkins CR, Conn PJ, Lindsley CW. Heterobiaryl and heterobiaryl ether derived M<sub>5</sub> positive allosteric modulators. *Bioorg Med Chem Lett*. 2010; 20:5617–5622. [PubMed: 20801651]
27. Liu J, Schoneberg T, van Rhee M, Wess J. Mutational analysis of the relative orientation of transmembrane helices I and VII in G protein-coupled receptors. *J Biol Chem*. 1995; 270:19532–19539. [PubMed: 7642637]
28. Bohme TM, Keim C, Dannhardt G, Mutschler E, Lambrecht G. Design and pharmacology of quinuclidine derivatives as M<sub>2</sub>-selective muscarinic receptor ligands. *Bioorg Med Chem Lett*. 2001; 11:1241–1243. [PubMed: 11354386]
29. Bohme TM, Augelli-Szafran CE, Hallak H, Pugsley T, Serpa K, Schwarz RD. Synthesis and pharmacology of benzoxazines as highly selective antagonists at M(4) muscarinic receptors. *J Med Chem*. 2002; 45:3094–3102. [PubMed: 12086495]
30. Choppin A, Stepan GJ, Loury DN, Watson N, Eglén RM. Characterization of the muscarinic receptor in isolated uterus of sham operated and ovariectomized rats. *Br J Pharmacol*. 1999; 127:1551–1558. [PubMed: 10455309]
31. Wang Y, Chackalamannil S, Hu Z, Greenlee WJ, Clader J, Boyle CD, Kaminski JJ, Billard W, Binch H 3rd, Crosby G, Ruperto V, Duffy RA, Cohen-Williams M, Coffin VL, Cox KA, Grotz DE, Lachowicz JE. Improving the oral efficacy of CNS drug candidates: discovery of highly orally efficacious piperidinyl piperidine M<sub>2</sub> muscarinic receptor antagonists. *J Med Chem*. 2002; 45:5415–5418. [PubMed: 12459007]
32. Sagara Y, Sagara T, Uchiyama M, Otsuki S, Kimura T, Fujikawa T, Noguchi K, Ohtake N. Identification of a novel 4-aminomethylpiperidine class of M<sub>3</sub> muscarinic receptor antagonists and structural insight into their M<sub>3</sub> selectivity. *J Med Chem*. 2006; 49:5653–5663. [PubMed: 16970392]

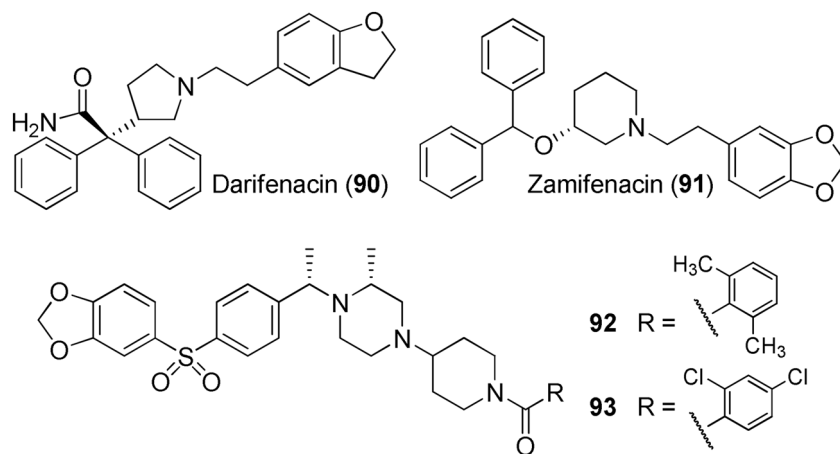
33. Augelli-Szafran CE, Blankley CJ, Jaen JC, Moreland DW, Nelson CB, Penrose-Yi JR, Schwarz RD, Thomas AJ. Identification and characterization of m1 selective muscarinic receptor antagonists. *J Med Chem.* 1999; 42:356–363. [PubMed: 9986705]
34. Solymar MFE, Fulop F. Enzyme-catalyzed kinetic resolution of piperidine hydroxy esters. *Tetrahedron: Asymmetry.* 2004; 15:3281–3287.
35. Inokuchi E, Narumi T, Niida A, Kobayashi K, Tomita K, Oishi S, Ohno H, Fujii N. Efficient synthesis of trifluoromethyl and related trisubstituted alkene dipeptide isosteres by palladium-catalyzed carbonylation of amino acid derived allylic carbonates. *J Org Chem.* 2008; 73:3942–3945. [PubMed: 18412390]
36. Anagnostaras SG, Murphy GG, Hamilton SE, Mitchell SL, Rahnama NP, Nathanson NM, Silva AJ. Selective cognitive dysfunction in acetylcholine M1 muscarinic receptor mutant mice. *Nat Neurosci.* 2003; 6:51–58. [PubMed: 12483218]
37. Gerber DJ, Sotnikova TD, Gainetdinov RR, Huang SY, Caron MG, Tonegawa S. Hyperactivity, elevated dopaminergic transmission, and response to amphetamine in M<sub>1</sub> muscarinic acetylcholine receptor-deficient mice. *Proc Natl Acad Sci U S A.* 2001; 98:15312–15317. [PubMed: 11752469]
38. Naito R, Yonetoku Y, Okamoto Y, Toyoshima A, Ikeda K, Takeuchi M. Synthesis and antimuscarinic properties of quinuclidin-3-yl 1,2,3,4-tetrahydroisoquinoline-2-carboxylate derivatives as novel muscarinic receptor antagonists. *J Med Chem.* 2005; 48:6597–6606. [PubMed: 16220976]
39. Choppin A, Eglen RM, Hegde SS. Pharmacological characterization of muscarinic receptors in rabbit isolated iris sphincter muscle and urinary bladder smooth muscle. *Br J Pharmacol.* 1998; 124:883–888. [PubMed: 9692772]
40. McCombie SW, Lin SI, Tagat JR, Nazareno D, Vice S, Ford J, Asberom T, Leone D, Kozlowski JA, Zhou G, Ruperto VB, Duffy RA, Lachowicz JE. Synthesis and structure-activity relationships of M(2)-selective muscarinic receptor ligands in the 1-[4-(4-arylsulfonyl)-phenylmethyl]-4-(4-piperidinyl)-piperazine family. *Bioorg Med Chem Lett.* 2002; 12:795–798. [PubMed: 11859005]
41. Watson N, Daniels DV, Ford APDW, Eglen RM, Hegde SS. Comparative pharmacology of human muscarinic M<sub>3</sub> and M<sub>5</sub> cholino-ceptors expressed in Chinese hamster ovary (CHO) cells. *Br J Pharmacol.* 1998; 123:U153–U153.
42. Pulido-Rios MT, Steinfeld T, Armstrong S, Watson N, Choppin A, Eglen R, Hegde SS. In vitro isolated tissue functional muscarinic receptor assays. *Curr Protoc Pharmacol.* 2010; Chapter 4(Unit 4):15. [PubMed: 22294371]
43. Zhang W, Yamada M, Gomeza J, Basile AS, Wess J. Multiple muscarinic acetylcholine receptor subtypes modulate striatal dopamine release, as studied with M<sub>1</sub>-M<sub>5</sub> muscarinic receptor knock-out mice. *J Neurosci.* 2002; 22:6347–6352. [PubMed: 12151512]
44. Kruse AC, Hu J, Pan AC, Arlow DH, Rosenbaum DM, Rosemond E, Green HF, Liu T, Chae PS, Dror RO, Shaw DE, Weis WI, Wess J, Kobilka BK. Structure and dynamics of the M3 muscarinic acetylcholine receptor. *Nature.* 2012; 482:552–556. [PubMed: 22358844]
45. Cheng Y, Prusoff WH. Relationship between the inhibition constant (K<sub>i</sub>) and the concentration of inhibitor which causes 50 per cent inhibition (I<sub>50</sub>) of an enzymatic reaction. *Biochem Pharmacol.* 1973; 22:3099–3108. [PubMed: 4202581]
46. Dvoskin LP, Zahniser NR. Robust modulation of [<sup>3</sup>H]dopamine release from rat striatal slices by D-2 dopamine receptors. *J Pharmacol Exp Ther.* 1986; 239:442–453. [PubMed: 3772803]
47. Zumstein A, Karduck W, Starke K. Pathways of dopamine metabolism in the rabbit caudate nucleus in vitro. *Naunyn Schmiedebergs Arch Pharmacol.* 1981; 316:205–217. [PubMed: 7254365]
48. Huang X, Zheng G, Zhan CG. Microscopic binding of M<sub>5</sub> muscarinic acetylcholine receptor with antagonists by homology modeling, molecular docking, and molecular dynamics simulation. *J Phys Chem B.* 2012; 116:532–541. [PubMed: 22185605]
49. Morris GMG, Halliday DS, Huey RS, Hart RWE, Belew RK, Olson AJ. Automated docking using a Lamarckian genetic algorithm and empirical binding free energy function. *J Comput Chem.* 1998; 19:1639–1662.



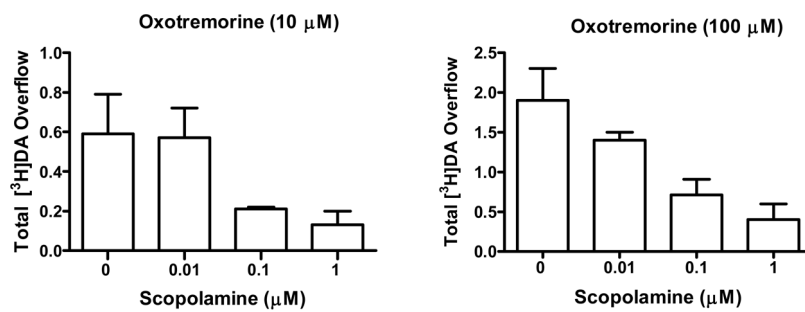
**Figure 1.**  
Structures of selected mAChR antagonists and their literature reported mAChR affinity data.



**Figure 2.**  
General structural modification strategy.

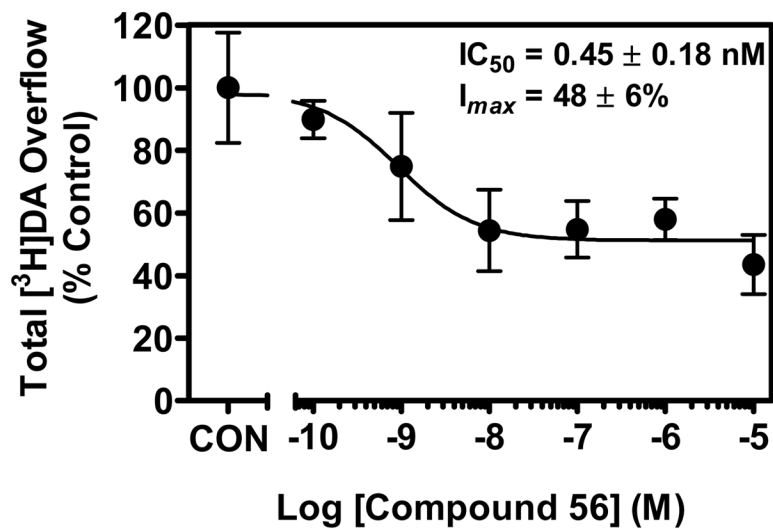


**Figure 3.** Structures of Darifenacin (90), Zamifenacin (91), and compounds 92 and 93.

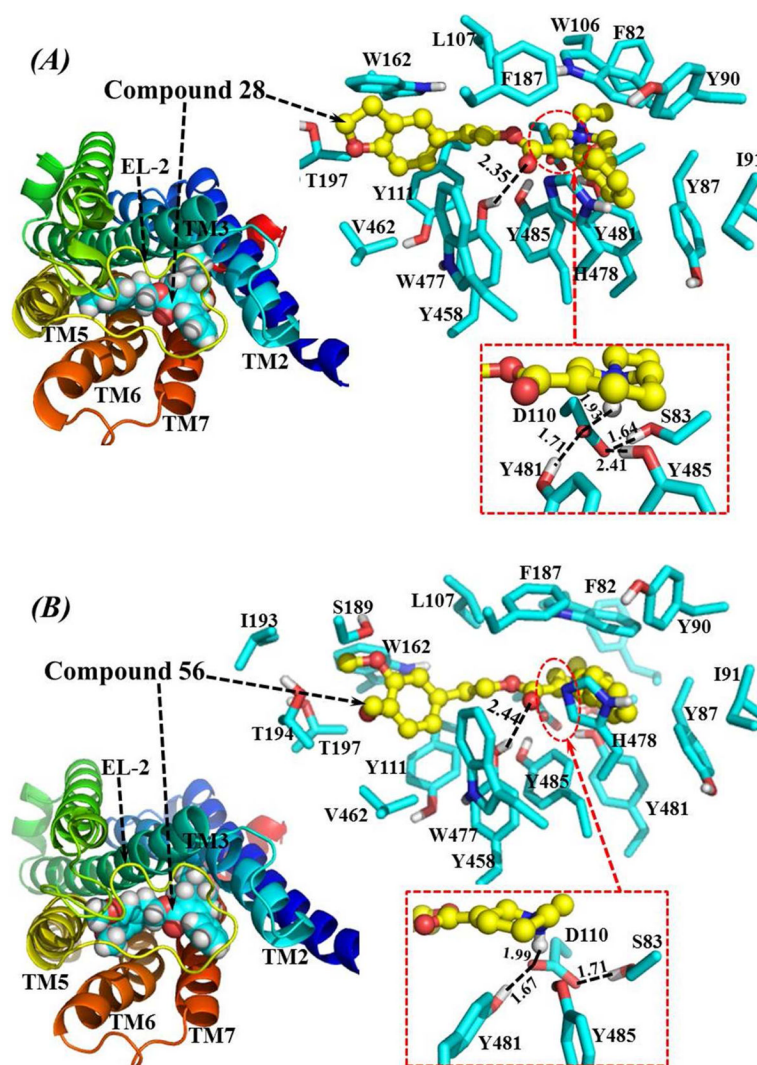


**Figure 4.** Scopolamine (0.01–1 μM) inhibits oxotremorine (10 μM and 100 μM) evoked [<sup>3</sup>H]DA release from rat striatal slices (data are expressed as Mean ± SEM, n = 3).

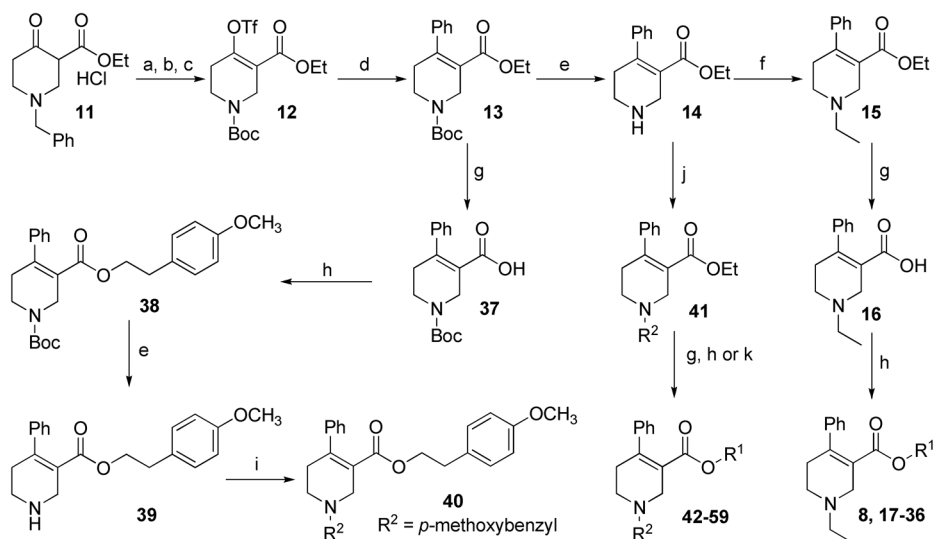




**Figure 5.** Compound **56** inhibits oxotremorine (100 μM) evoked [<sup>3</sup>H]DA release from rat striatal slices (data are expressed as Mean ± SEM, n = 4).

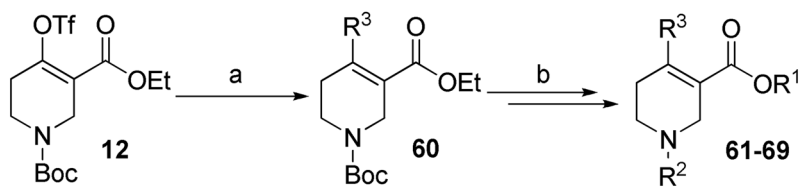


**Figure 6.** Homology model of human M<sub>5</sub> mAChR based on the X-ray crystal structure of rat M<sub>3</sub> mAChR (PDB entry of 4DAJ at 3.4 Å resolution, A chain). (A) Top view on the energy-minimized binding structure of M<sub>5</sub> mAChR-Compound **28** complex. (B) Top view on the energy-minimized binding structure of M<sub>5</sub> mAChR-Compound **56** complex. The receptor proteins in (A) and (B) are represented as ribbon in rainbow color, and compound **28** and **56** are shown as spheres (left panel) or ball-and-stick (right panel). Residues within 5 Å of compound **28** and **56** are labeled and shown in stick. **28** and **56** have very similar hydrogen bonding interactions with the protein, including interactions between the D110 side chain and the cationic heads of the compounds, interactions between the carbonyl oxygen atoms of the compounds and the Y458 side chain, and the interactions among side chains of D110, S83, Y481 and Y485. These hydrogen bonding interactions are shown in dashed lines along with the labeled distances.

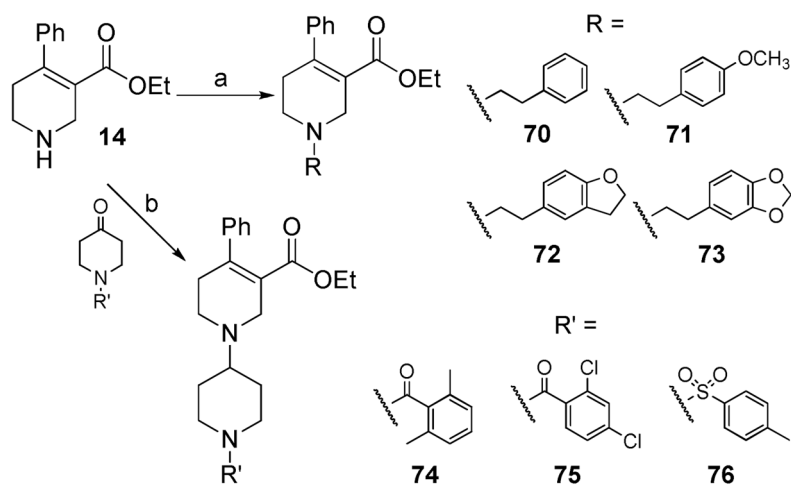


**Scheme 1. Synthesis of Compounds 8, 17–36, 40, and 42–59<sup>a</sup>**

<sup>a</sup>Reagents and conditions: (a) H<sub>2</sub>, 10% Pd/C (5 w/w%), EtOH; (b) (BOC)<sub>2</sub>O, Et<sub>3</sub>N, CH<sub>2</sub>Cl<sub>2</sub>; (c) Tf<sub>2</sub>O, *i*Pr<sub>2</sub>NH, CH<sub>2</sub>Cl<sub>2</sub>, -78 °C; (d) PhB(OH)<sub>2</sub>, Pd(PPh<sub>4</sub>)<sub>3</sub>, Na<sub>2</sub>CO<sub>3</sub> (2.0 M), THF, 65 °C; (e) TFA/CH<sub>2</sub>Cl<sub>2</sub> (1:1); (f) EtI, K<sub>2</sub>CO<sub>3</sub>, EtOH; (g) 10% KOH (aq.)/EtOH (1:1); (h) alcohols, EDCI, DMAP, CH<sub>2</sub>Cl<sub>2</sub>; (i) *p*-methoxybenzaldehyde, NaBH(OAc)<sub>3</sub>, HOAc, THF; (j) aldehydes, NaBH<sub>3</sub>CN, EtOH; (k) alcohols, 2,4,6-trichlorobenzoyl chloride, DMAP, Et<sub>3</sub>N, THF.

**Scheme 2. Synthesis of Compounds 61–69<sup>a</sup>**

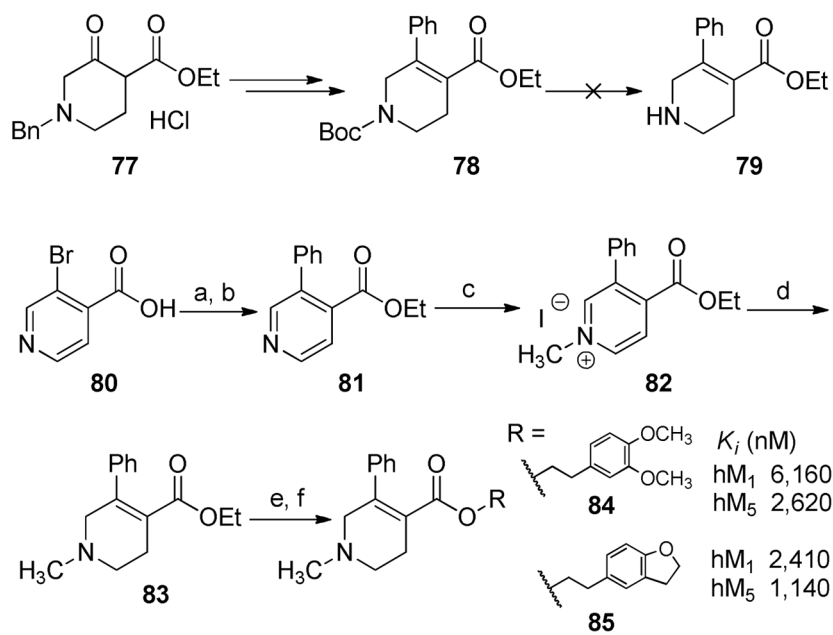
<sup>a</sup>Reagents and conditions: (a) substituted phenylboronic acids, Pd(PPh<sub>4</sub>)<sub>3</sub>, Na<sub>2</sub>CO<sub>3</sub> (2.0 M), THF, 65 °C; (b) same as from compound 13 to 42 in Scheme 1.



70-76, not active at hM<sub>1</sub> and hM<sub>5</sub> ( $K_i > 100,000$  nM)

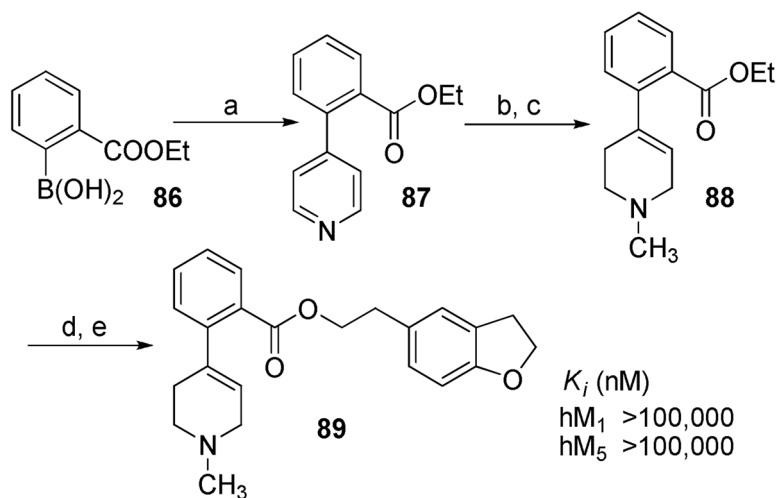
**Scheme 3. Synthesis of Compounds 70–76<sup>a</sup>**

<sup>a</sup>Reagents and conditions: (a) alkyl bromides, KI, K<sub>2</sub>CO<sub>3</sub>, CH<sub>3</sub>CN, reflux; (b) NaBH(OAc)<sub>3</sub>, HOAc, THF, 65 °C for **74**, rt for **75** and **76**.



**Scheme 4. Synthesis of Compounds 84 and 85<sup>a</sup>**

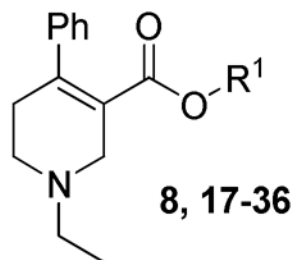
<sup>a</sup>Reagents and conditions: (a) EtOH, H<sub>2</sub>SO<sub>4</sub> (con.), reflux; (b) PhB(OH)<sub>2</sub>, Pd(PPh<sub>4</sub>)<sub>3</sub>, Na<sub>2</sub>CO<sub>3</sub> (2.0 M), THF, 65 °C; (c) MeI, acetone; (d) NaBH<sub>4</sub>, EtOH; (e) 10% KOH (H<sub>2</sub>O)/EtOH (1:1); (f) alcohols, EDCl, DMAP, CH<sub>2</sub>Cl<sub>2</sub>.

**Scheme 5. Synthesis of Compound 89<sup>a</sup>**

<sup>a</sup>Reagents and conditions: (a) 4-bromopyridine, Pd(PPh<sub>3</sub>)<sub>4</sub>, Na<sub>2</sub>CO<sub>3</sub> (2.0 M), THF, 65 °C; (b) MeI, acetone; (c) NaBH<sub>4</sub>, EtOH; (d) 10% KOH (H<sub>2</sub>O)/EtOH (1:1); (e) 2-(2,3-dihydrobenzofuran-5-yl)ethanol, EDCI, DMAP, CH<sub>2</sub>Cl<sub>2</sub>.

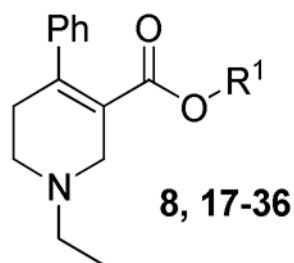
**Table 1**

Structures and Binding Affinity for Scopolamine (1), Compounds 8, and 17–36 at the  $hM_1$  and  $hM_5$  mAcChRs<sup>a</sup>

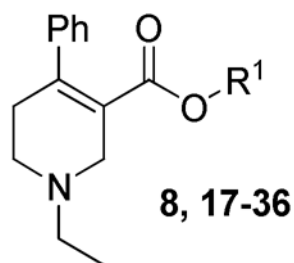


compd	R <sup>1</sup>	<i>K<sub>i</sub></i> , nM		
		<i>hM</i> <sub>1</sub>	<i>hM</i> <sub>5</sub>	<i>hM</i> <sub>1</sub> / <i>hM</i> <sub>5</sub>
1	-	7.5	17.6	0.4
8		170	420	0.4
17		1,730	1,250	1.4
18		470	150	3.1
19		3,060	3,610	0.8
20		3,290	470	7.0
21		>100,000	>100,000	-

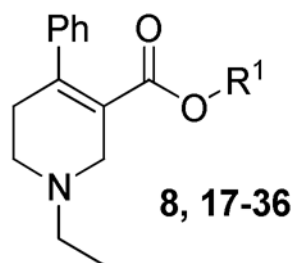




compd	R <sup>1</sup>	K <sub>i</sub> , nM		
		hM <sub>1</sub>	hM <sub>5</sub>	hM <sub>1</sub> /hM <sub>5</sub>
22		200	290	0.7
23		100	190	0.5
24		560	410	1.4
25		240	370	0.6
26		810	440	1.8
27		>100,000	>100,000	-
28		1,390	230	6.0



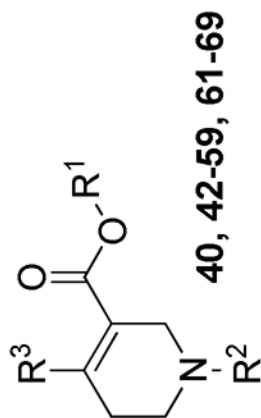
compd	R <sup>1</sup>	K <sub>i</sub> , nM		
		hM <sub>1</sub>	hM <sub>5</sub>	hM <sub>1</sub> /hM <sub>5</sub>
29		200	280	0.7
30		60	120	0.5
31		11,700	2,460	4.8
32		>100,000	>100,000	-
33		>100,000	>100,000	-
34		410	760	0.5
35		370	140	2.6



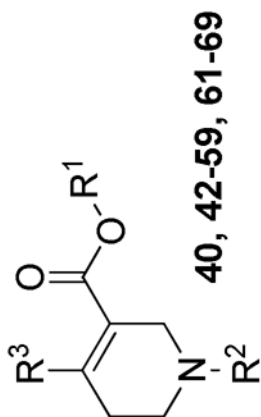
compd	R <sup>1</sup>	K <sub>i</sub> , nM		
		hM <sub>1</sub>	hM <sub>5</sub>	hM <sub>1</sub> /hM <sub>5</sub>
36		140	190	0.7

<sup>a</sup>At least three independent experiments with samples evaluated in duplicate were performed to obtain the K<sub>i</sub> value.

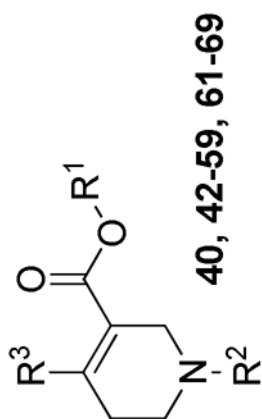
Table 2

Structures and Binding Affinity for Analogues 40, 42–59, and 61–69 at the hM<sub>1</sub> and hM<sub>5</sub> mAcChRs<sup>a</sup>

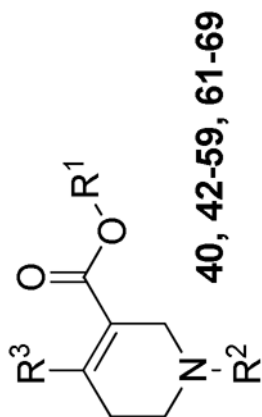
compd	R <sup>1</sup>	R <sup>2</sup>	R <sup>3</sup>	K <sub>i</sub> , nM		
				hM <sub>1</sub>	hM <sub>5</sub>	hM <sub>1</sub> /hM <sub>5</sub>
40		4-MeO-Bn	Ph	>100,000	>100,000	-
42	<i>ibid.</i>	Me	Ph	20	30	0.7
43	<i>ibid.</i>	<i>n</i> Pr	Ph	>100,000	>100,000	-
44	<i>ibid.</i>	<i>n</i> Bu	Ph	>100,000	>100,000	-
45		Me	Ph	290	60	4.8
46	<i>ibid.</i>	<i>n</i> Pr	Ph	>100,000	>100,000	-
47	<i>ibid.</i>	<i>n</i> Bu	Ph	>100,000	>100,000	-
48		Me	Ph	5,400	1,160	4.7



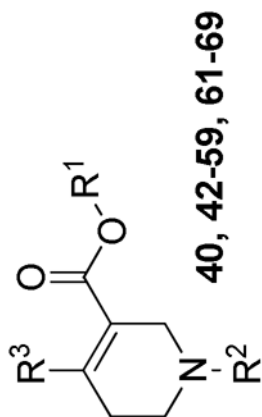
compd	R <sup>1</sup>	R <sup>2</sup>	R <sup>3</sup>	K <sub>b</sub> , nM		
				hM <sub>1</sub>	hM <sub>5</sub>	hM <sub>1</sub> /hM <sub>5</sub>
49		Me	Ph	>100,000	>100,000	-
50		Me	Ph	920	630	1.5
51		Me	Ph	340	190	1.8
52		Me	Ph	510	110	4.6
53		Me	Ph	880	280	3.1



compd	$R^1$	$R^2$	$R^3$	$K_b$ , nM		
				$hM_1$	$hM_5$	$hM_1/hM_5$
54		Me	Ph	330	80	4.1
55		Me	Ph	2,700	740	3.6
56		Me	Ph	25,300	2,240	11.3
57		Me	Ph	24,400	5,040	4.8



compd	R <sup>1</sup>	R <sup>2</sup>	R <sup>3</sup>	K <sub>i</sub> , nM		
				hM <sub>1</sub>	hM <sub>5</sub>	hM <sub>1</sub> /hM <sub>5</sub>
58		Me	Ph	>100,000	>100,000	-
59		Me	Ph	6,190	3,070	2.0
61		Et	4-F-Ph	7,900	2,350	3.4
62	<i>ibid.</i>	Me	3-F-Ph	>100,000	>100,000	-
63	<i>ibid.</i>	Me	2-F-Ph	5,270	740	7.0
64	<i>ibid.</i>	Me	3-MeO-Ph	2,430	2,680	0.9
65	<i>ibid.</i>	Me	2-MeO-Ph	8,350	2,410	3.5



compd	R <sup>1</sup>	R <sup>2</sup>	R <sup>3</sup>	K <sub>i</sub> , nM		
				hM <sub>1</sub>	hM <sub>5</sub>	hM <sub>1</sub> /hM <sub>5</sub>
<b>66</b>		Me	3-F-Ph	27,000	3,340	8.1
<b>67</b>	<i>ibid.</i>	Me	2-F-Ph	>100,000	>100,000	-
<b>68</b>	<i>ibid.</i>	Me	3-MeO-Ph	>100,000	>100,000	-
<b>69</b>	<i>ibid.</i>	Me	2-MeO-Ph	>100,000	>100,000	-

<sup>a</sup> At least three independent experiments with samples evaluated in duplicate were performed to obtain the K<sub>i</sub> value.



**Table 3**  
Binding Affinity and Selectivity for Selected Analogues at the hM<sub>1</sub>-hM<sub>5</sub>mAcChRs<sup>a</sup>

Compd	$K_i$ , nM					
	hM <sub>5</sub>	hM <sub>1</sub> (M <sub>1</sub> /M <sub>5</sub> ) <sup>b</sup>	hM <sub>2</sub> (M <sub>2</sub> /M <sub>5</sub> ) <sup>b</sup>	hM <sub>3</sub> (M <sub>3</sub> /M <sub>5</sub> ) <sup>b</sup>	hM <sub>4</sub> (M <sub>4</sub> /M <sub>5</sub> ) <sup>b</sup>	
1	17.6	7.5 (0.4)	9.5 (0.5)	6.5 (0.4)	36.9 (2.1)	
8	420	170 (0.4)	1,100 (2.6)	1,370 (3.3)	1,730 (4.1)	
20	470	3,290 (7.0)	2,030 (4.3)	4,070 (8.7)	11,500 (24)	
28	230	1,390 (6.0)	>100,000 (>435)	31,100 (135)	10,500 (46)	
45	60	290 (4.8)	1,170 (20)	2,840 (47)	1,890 (32)	
56	2,240	25,300 (11)	>100,000 (>45)	>100,000 (>45)	>100,000 (>45)	
57	5,040	24,400 (4.8)	>100,000 (>20)	>100,000 (>20)	>100,000 (>20)	
63	740	5,270 (7.1)	540 (0.7)	4,890 (6.6)	5,740 (7.8)	
66	3,340	27,000 (8.0)	>100,000 (>30)	>100,000 (>30)	>100,000 (>30)	

<sup>a</sup> At least three independent experiments with samples evaluated in duplicate were performed to obtain the  $K_i$  value;

<sup>b</sup> Numbers in the parentheses are the ratios of binding affinity between M<sub>5</sub> and the respective subtype.